Reaction Kinetics, Mechanisms and Catalysis (2020) 129:403–419
https://doi.org/10.1007/s11144-019-01708-4

Ni,Co/SiO_2 and Ni/SiO_2,Co bimetallic microsphere catalysts indicating high activity and stability in the dry reforming of methane

Gamze Gunduz-Meric[1] · Suleyman Kaytakoglu[2] · Levent Degirmenci[1]

Received: 15 October 2019 / Accepted: 9 December 2019 / Published online: 14 December 2019

Abstract

Two separate synthesis procedures were applied to alter the location of Cobalt (Co) in bimetallic silica (SiO_2) microsphere catalyst with Nickel (Ni) as the second active metal. Co was either encapsulated with simultaneous Ni addition inside core structure (Ni,Co/SiO_2) or impregnated on the shell following initial encapsulation of Ni inside the microsphere (Ni/SiO_2&Co). Catalysts were tested in dry reforming of methane (DRM) reaction at 750 °C with a feed mixture of CH_4:CO_2:N_2 = 1:1:1. Reactions were performed in a stainless steel temperature-controlled tube reactor. Results indicated the highest activity values with 4Ni-1Co ratio in catalyst structure and Co impregnated on catalyst structure revealed higher activity for all loadings compared to Ni,Co/SiO_2 catalysts. CH_4 and CO_2 conversions for 3 h of reaction were obtained as 87 and 94%, and H_2/CO ratio was determined as 0.84 in the presence of Ni/SiO_2&Co catalyst with 4Ni-1Co loading. Coke formation was not detected for the catalyst with 4Ni-1Co loading and the highest coke amount was 2% among all catalysts. Time on stream test in the presence of Ni/SiO_2&Co catalyst with 4Ni-1Co loading was conducted for 12 h in identical conditions, and results revealed a stable activity with conversions equal to 3 h of reaction. Coke suppression during DRM reaction was attributed to microsphere structure, Co presence and SiC formation. SiC formation was introduced as a unique situation emanated as a result of the reaction between SiO_2 and C.

Keywords Dry reforming · Core–shell microsphere · Nickel–cobalt · Hydrogen production · Sol–gel microencapsulation

Electronic supplementary material The online version of this article (https://doi.org/10.1007/s11144-019-01708-4) contains supplementary material, which is available to authorized users.

✉ Levent Degirmenci
levent.degirmenci@bilecik.edu.tr

[1] Department of Chemical Engineering, Bilecik Seyh Edebali University, 11200 Bilecik, Turkey

[2] Department of Chemical Engineering, Eskisehir Technical University, 26555 Eskisehir, Turkey

Introduction

Dry reforming of methane (DRM) reaction (1)

$$CH_4 + CO_2 \rightarrow 2CO + 2H_2 \quad (1)$$

was previously applied in the production of synthesis gas with hydrogen/carbon monoxide (H_2/CO) ratio close to 1 [1–3]. It is possible to use natural gas resources with high carbon dioxide (CO_2) content via DRM reaction.[4]. Besides, the reaction is a good alternative in preventing expensive and complex gas separation processes and provides a different approach for the use of biogas. Methane (CH_4) and CO_2 are obtained in ratios ranging from 40 to 70% for CH_4 and 30 to 60% for CO_2, as a result of anaerobic decomposition of biomass [5]. The reaction is essential as it contributes to the consumption of these well-known greenhouse gases [6].

Decomposition of CH_4 (2), the "Boudouard" reaction (3), and the reverse water gas shift reaction (4) are significant side reactions decreasing the efficiency of the process [7–9]. Reverse water gas shift reaction affects product distribution by introducing additional CO to the process decreasing H_2/CO ratio below 1. Decomposition of CH_4 is another setback of the process causing coke formation which, in the short term, reduces the catalytic activity. Coke deposition on the catalyst surface causes suppression of catalytic activity and blockage of the reactor which often results in termination of reaction [10]. Nickel (Ni), Cobalt (Co) and Iron (Fe) are the known metals that give high activity for this reaction [11]. However, the main problem of Co and Ni containing catalysts is that they lose their activity due to coke formation. This coke layer covers the active regions of the catalyst causing its deactivation as the reaction progresses [12, 13].

$$CH_4 \rightarrow C + 2H_2 \quad \Delta H^{\circ}_{298} = 75.2 \text{ kJ mol}^{-1} \quad (2)$$

$$2CO \rightarrow C + CO_2 \quad \Delta H^{\circ}_{298} = -173.0 \text{ kJ mol}^{-1} \quad (3)$$

$$CO_2 + H_2 \leftrightarrow CO + H_2O \quad \Delta H^{\circ}_{298} = 41.2 \text{ kJ mol}^{-1} \quad (4)$$

Properties of the support material of the catalyst [14–16], metal composition [17, 18], and catalyst preparation method [19] were recently investigated in literature with fine results in terms of catalyst activity and stability. Different approaches have also been developed to maintain a synergy between the two metals, including optimization of Co, Ni composition, and addition of fine metals such as Ruthenium (Ru), Platinium (Pt), and Palladium (Pd) [20–23]. Lanthanum (La) was recently utilized in the work of Silva et al. [24]. to induce the formation of $LaNiO_3$ perovskites. The interaction between La and Ni decreased the sintering of the active phase and increased the degree of active metal dispersion throughout catalyst surface. MgO was utilized in another study as an additive on Co/SiO_2 catalysts. The addition of high MgO amounts (30–35%) in silicate structure resulted in the formation of a $MgSiO_4$ adlayer, which improved stability of the catalyst under severe conditions [25].

Silica supports in various forms have been introduced to improve the stability of the catalyst and to increase resistance to carbon deposition during reaction [26–28]. These forms included KIT-6, SBA-15 and lately core–shell structures with active metal inside the support. Ni and yttrium (Y) promoted KIT-6 catalysts revealed H_2/CO ratios close to stoichiometric ratios during the DRM reaction conducted in a temperature interval of 600–750 °C [26]. Ni and Co were added on SBA-15 by wet impregnation method in the work of Erdogan et.al.[27]. Catalysts, utilized in dry reforming of methane reaction, gave promising results. Co addition on the structure induced formation of Ni-Co alloy which inhibited Ni agglomeration on catalyst surface [27]. In a study conducted by Al-Fatesh et.al.[28], SBA-15 structure was modified with Magnesium (Mg), La, and Scandium (Sc) employed as promoters. Results indicated a 26% increase in the case of Mg addition, while a 28% increase of activity was achieved with Sc addition on catalysts structure [28]. Core–shell catalysts containing silica-coated active metal were successfully utilized in DRM reaction. These structures indicated better coke resistance and sustainability compared to uncoated metal catalysts [29].

Silicon carbide (SiC) formation was determined on Ni-based silica microspheres in our previous studies. Results indicated that the carbon, formed during the reaction, had been utilized to form SiC during DRM reaction. Utilization of carbon to form SiC gained the catalyst a self-cleaning property of the active sites, and complete elimination of coke on the active sites was achieved for the investigated time interval [30, 31]. The present study included Co addition on the structure to increase both catalyst activity and resistance towards coke formation. Co, as the only source of active material, indicated poor catalytic performance in syngas production. On the other hand, the addition of small amounts of Co to Ni increased catalytic activity due to the synergic effect between these metals [32]. Co presence in catalyst structure was reported to suppress metal sintering and carbon deposition [32, 33].

Bimetallic silica microspheres containing Co and Ni were synthesized with an average particle diameter of 400 nm. These were tested in dry reforming of methane reaction. Ni and Co were added to catalyst structure in varying amount and the total metallic content of the catalysts was kept at 5%. Two synthesis procedures were employed to maintain Ni and Co both in the core or Ni in the core and Co on the shell side of the catalyst. Regulation of the metal compositions and Co placement in a microsphere structure were adopted as new approaches to increase the activity and stability of the catalyst during reaction [34].

Material and methods

Ni–Co encapsulation in the core of silica microsphere

Sol–gel microencapsulation method, used in our previous studies, was applied in the present study with slight modifications [30, 35]. The method includes sequential preparation and mixing of oil and water phases to obtain microspheres. Oil phase was formed by addition of ammonia to ethanol. Resulting solution was homogenized at 5000 rpm for 5 min. Water phase consisted of hexadecyl cetyl trimethyl

ammonium bromide used as a surfactant (CTAB, Merck) and metal salts dissolved in de-ionized water. Ni and Co were utilized as active metals of the catalyst and their total amounts were adjusted as 5% of total silicium weight. $Ni(NO_3)_2{\cdot}6H_2O$ (Sigma-Aldrich) and $CoCl_2{\cdot}6H_2O$ (Sigma-Aldrich) were utilized as Ni and Co sources. Ni-M (M:Co) ratio was altered as 1-1, 1-2, 2-1 and 4-1, respectively. The water phase and oil phase were mixed and re-suspended in homogenizer at 5000 rpm for 5 min. Tetraethylortho silicate (TEOS, Merck) was added slowly to this resulting solution and stirred mechanically at 300 rpm for 6 h. The solid sample was dried at room temperature (24 h) after applying washing steps with ethanol and de-ionized water. Catalyst preparation was finalized following a sequential procedure of calcination (6 h) and H_2 treatment (1 h) at 750 °C. Catalysts were named as $Ni,Co/SiO_2$ to prevent confusion.

Silica microspheres obtained by encapsulation of Ni in the core and impregnation of Co on the shell side

A two-step procedure was followed in the preparation of the catalyst. Initially, microspheres with a designated amount of Ni was prepared by encapsulation procedure identical to that followed in the preparation of Ni-Co silica microspheres. Ni containing silica microspheres was washed, dried at room temperature and calcined at 750 °C. Co addition was achieved by the dropwise addition of its precursor solution (25 ml) to Ni silica microsphere which was dispersed in 25 ml of de-ionized water. The resulting solution was stirred at 40 °C and 300 rpm for 24 h in order to remove water. The final product was obtained after drying at room temperature, re-calcination and H_2 treatment (1 h) at 750 °C. Metal loadings (Ni–Co ratio) were identical for both procedures. These catalysts were denoted as Ni/SiO_2&Co to maintain easy follow-up.

Catalysts characterization

Characterization studies were conducted in the presence of both fresh and spent catalysts to evaluate the effect of applied reaction conditions on the structure. X-ray diffraction patterns (XRD) of the catalysts were obtained by a Panalytical Empyrean instrument at 200 kV and 50 mA with 2θ values ranging between 5° and 80° and with a speed of 10 °C min^{-1}. Nitrogen adsorption–desorption isotherms, BET surface area, pore volume and pore size distributions of the catalysts were obtained via Micromeritics ASAP instrument. Surface morphology was determined using the Quanta 400F Field Emission SEM device. Metal loadings of Ni and Co were analyzed by ICP-OES using a Perkin Elmer DRC II device. XRD and SEM analyses were also performed with used catalysts along with Thermogravimetric analyses (TGA, Perkin Elmer Pyris1) and Raman Spectroscopy measurements (Bruker FRA 106/S). The aim was to determine structural changes and coke formation during reaction. XRD analyses with spent catalysts were conducted to exclusively validate the presence of SiC after reaction [30, 31]. Before XRD analyses, spent catalyst samples were treated with nitrogen (N_2) at 1200 °C for 16 h with the intent

of converting amorphous silica to crystal β-form [31]. The aim of this temperature treatment was to enable visualization of SiC in its crystal form since amorphous SiC formation was generally observed below 1400 °C [30, 31]. SiC was likely to be found at 750 °C, which was the designated temperature for calcination, reduction and reaction. TGA analyses were performed in the presence of airflow, in a temperature range of 25–900 °C and at a heating rate of 10 °C min^{-1}. The type of possible carbon deposition of spent catalysts was determined by Raman spectroscopy device equipped with a 532 nm laser.

Catalytic activity measurements

DRM was selected as the model reaction to evaluate the activity and stability of the catalysts. Reactions were performed in the presence of 0.1 g catalyst loading under atmospheric pressure. Reactions were performed at the same temperature and catalysts were screened for 3 h in a fixed bed reactor fitted inside a steel tube. As previously mentioned, catalysts were reduced under 20 ml min^{-1}. H_2 flow at 750 °C for 1 h. Reduction procedure and reaction experiments were performed consecutively to avoid interaction of the catalysts with atmosphere and prevent activity losses due to metal oxidation. Reactant and product streams were analyzed on-line by gas chromatography (HP 6890 Series), equipped with a thermal conductivity detector (TCD) and "Poropak Q" and "HayeSep N" columns. N_2 was used both as the carrier and reference gas and the reactant stream consisted of a mixture of CH_4 (20 ml/min.), CO_2 (20 ml min^{-1}) and N_2 (20 ml min^{-1}). This mixture was transferred to the reactor with a space velocity of 36,000 ml $(g_{cat}\ h)^{-1}$. Stability test of the catalyst with the highest activity was also performed in identical conditions [750 °C, CH_4:CO_2:N_2 = 1:1:1, 0.1 g catalyst loading and WHSV: 36,000 ml $(gcat\ h)^{-1}$] for 12 h.

The conversions of CH_4 and CO_2, the selectivity of H_2 and CO and H_2/CO ratio were calculated as follows [36]:

$$CH_4 \text{ conversion } (\%) = \frac{[\text{moles } CH_4] \text{ in} - [\text{moles } CH_4] \text{ out}}{[\text{moles } CH_4] \text{in}} \times 100 \tag{5}$$

$$CO_2 \text{ conversion } (\%) = \frac{[\text{moles } CO_2] \text{ in} - [\text{moles } CO_2] \text{ out}}{[\text{moles } CO_2] \text{ in}} \times 100 \tag{6}$$

$$H_2 \text{ selectivity} = \frac{[\text{moles } H_2]}{[\text{moles } CH_4] \text{ in} - [\text{moles } CH_4] \text{ out}} \tag{7}$$

$$CO \text{ selectivity} = \frac{[\text{moles CO}]}{[\text{moles } CH_4] \text{ in} - [\text{moles } CH_4] \text{ out}} \tag{8}$$

$$\frac{H_2}{CO} = \frac{\text{moles of } H_2 \text{ produced}}{\text{moles of CO produced}} \quad (9)$$

Results and discussion

Characterization results of fresh bimetallic Ni-Co microsphere catalysts

The specific surface areas, pore sizes and pore volumes of fresh bimetallic Ni-Co microsphere catalysts and metal loadings calculated from ICP-OES analyses were illustrated in Table 1. ICP-OES results, as seen from the table, indicated a severe loss of active metal during synthesis. A comparison of procedures revealed negligible preservation of metal loading in the case of Co impregnation. Results showed that a maximum of 3% could have been loaded with either of these procedures, and modification of the synthesis method in future works had been required to increase the yield.

All catalysts exhibited type IV isotherm with a hysteresis loop of H4-type according to IUPAC classification [37]. Those texture results describe narrow and slit-shaped pores that contain a considerable amount of micro-pores in all samples. Pore sizes were identical, indicating a mesoporous structure with bottom-line values as seen from Table 1. Nitrogen adsorption–desorption isotherms and pore size distributions of fresh catalysts were given in Supplementary File. A comparison of surface areas revealed higher values for Ni/SiO_2&Co catalysts, as expected. In the case of $Ni,Co/SiO_2$ catalysts, the decrease in surface areas and pore volumes implied incorporation of Ni and/or Co inside the pores. However, that should not be the case considering similar pore sizes for both (Ni/SiO_2&Co and $Ni,Co/SiO_2$) catalysts. Instead, metal dispersion was more likely to be centered near pores of microsphere structure.

XRD patterns obtained from catalysts with varying loading amounts were given in Fig. 1. These peaks were obtained for calcined catalysts before H_2 treatment. Peak

Table 1 Properties of fresh catalysts

Catalyst	BET surface area ($m^2\ g^{-1}$)	BJH ads. pore size (nm)	Pore volume ($cm^3\ g^{-1}$)	ICP-OES (Ni–Co %)
$Ni,Co/SiO_2$				
1Ni-1Co	234	3.3	0.2	1.46–1.75
1Ni-2Co	171	3.4	0.1	0.78–2.21
2Ni-1Co	102	3.2	0.1	1.84–1.15
4Ni-1Co	316	2.7	0.2	2.24–0.79
Ni/SiO_2&Co				
1Ni-1Co	401	2.9	0.3	1.44–2.01
1Ni-2Co	490	2.6	0.4	1.00–2.57
2Ni-1Co	458	2.6	0.3	2.01–1.28
4Ni-1Co	359	2.7	0.2	2.34–0.88

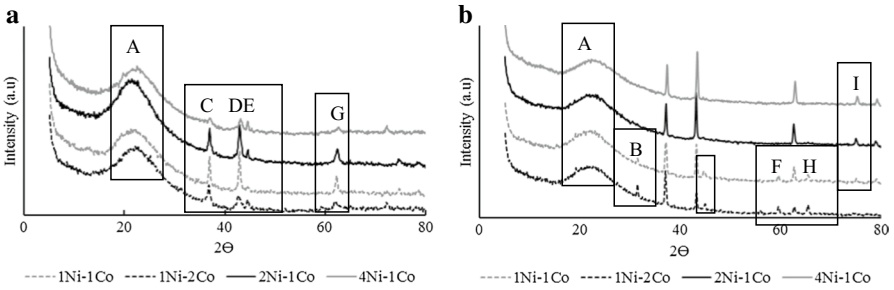

Fig. 1 XRD patterns of fresh **a** Ni,Co/SiO_2 synthesized by sol–gel microencapsulation with Ni and Co encapsulated in the core and **b** Ni/SiO_2&Co synthesized by sol–gel microencapsulation-impregnation with Ni encapsulated in the core, Co impregnated on the shell

values were coded with letters according to increasing peak values. Peaks obtained in the range of 2θ: 20°–30° for all catalysts (A) were originated from the amorphous structure of silica. The diffraction peaks observed at 2θ of 37.1°, 43.1° 62.6° (C,D,G) and 75° (I) showed the characteristic crystal NiO phase (Ref. Code 96–210-0647). These peaks existed in both catalysts, and peak value at 75° was an indicator unique to NiO formation in catalyst structure. Peak values obtained at 44.6 for all Ni,Co/SiO_2 catalysts could only be observed with 1Ni-1Co and 1Ni-2Co loadings of Ni/SiO_2&Co catalysts (E). (400) Planes of $NiCo_2O_4$ and $CoCo_2O_4$ indicated close peak values, hence overlapping of these peaks should be expected. Having said that, results could be interpreted as the formation of $NiCo_2O_4$ alloy for Ni,Co/SiO_2 catalysts, while results of Ni/SiO_2&Co catalysts implied the formation of $CoCo_2O_4$ structure due to high Co loadings. $CoCo_2O_4$ presence was validated with peak values obtained exclusively at 31.8°, 59.7° and 65.5° for Ni/SiO_2&Co catalysts (B,F,H) with increasing Co amounts in catalyst structure (Ref. Code 96–154-1643).

Comparison of intensity values between synthesis procedures indicated higher intensity of NiO crystals (C,D,G) when Co was impregnated on the surface. This high intensity was an expected result based on crystal sizes of both catalysts. Crystal sizes of NiO obtained in the presence of Ni,Co/SiO_2 and Ni/SiO_2&Co catalysts were calculated from Scherrer equation. These values were reported to be similar due to close lattice parameters [38]. Variation in Ni amount did not have a significant effect on crystal sizes due to low metal contents (around 3%). Average values were reported for both catalysts, as expected. On the other hand, it was still possible to compare crystal sizes based on the synthesis procedure. An average of 5.2 nm was determined in the case of Ni,Co/SiO_2 while crystal sizes were 7.9 nm for Ni/SiO_2&Co catalysts. Results revealed an evident decrease due to simultaneous Co addition, which should be expected during alloy formation [33]. SEM images validated microsphere formation for both catalysts (See Supplementary file).

DRM performance of catalysts

Activities of catalysts for the DRM reaction were illustrated in terms of CH_4 and CO_2 conversions (Fig. 2). CH_4 and CO_2 conversions varied as 4Ni-1Co

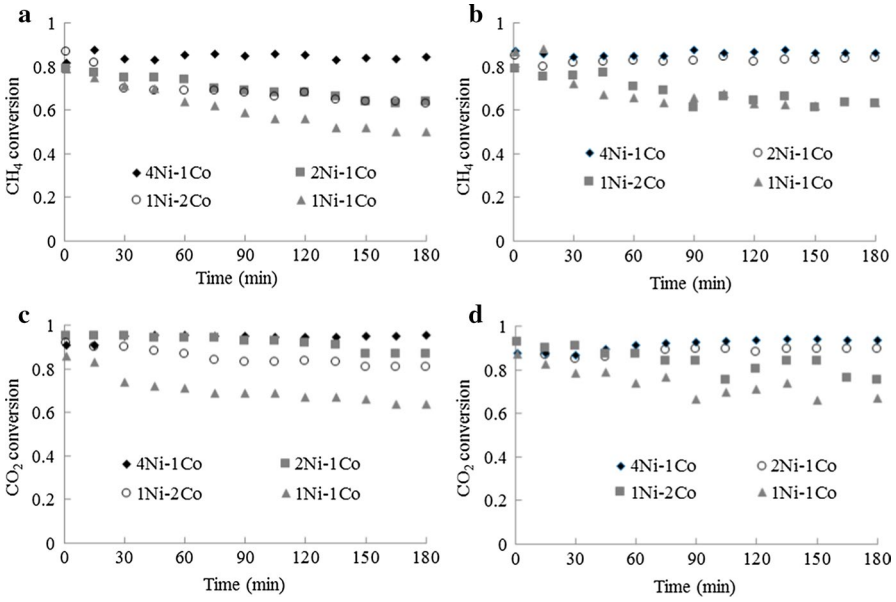

Fig. 2 The performance of Ni-Co bimetallic microsphere catalysts in DRM reaction at 750 °C, CH_4:CO_2:N_2 = 1:1:1, 0.1 g catalyst loading and WHSV:36,000 ml (gcat h)$^{-1}$ **a** CH_4, **c** CO_2 conversion in the presence of Ni,Co/SiO_2 and **b** CH_4, **d** CO_2 conversion in the presence of Ni/SiO_2&Co catalysts

(85.95%) > 2Ni-1Co (64.87%) > 1Ni-2Co (63.81) > 1Ni-1Co (50.64%)) in the presence of Ni,Co/SiO_2 catalysts for 3 h of reaction. Results showed a decrease in activity due to increasing Co amount in catalyst structure. Conversion values varied as 4Ni-1Co (87.94%) > 2Ni-1Co (84.90%) > 1Ni-2Co (63–75%) > 1Ni-1Co (63–67%) in the case of Co (Ni/SiO_2&Co) impregnation. In our previous study, the activity of Ni containing SiO_2 microspheres was investigated for DRM reaction, and the highest activity was obtained as 73 and 89% based on CH_4 and CO_2 conversions, respectively [23]. CO_2 conversions (Fig. 2b, d) was higher than CH_4 (Fig. 2a, c) conversions for both catalysts. This higher conversion was expected due to significant contribution of reverse water gas shift (RWGS) reaction occurred in the course of the dry reforming process.

Equilibrium conversions of CH_4 and CO_2 were previously calculated by Gaseq Chemical Equilibrium Programme in the presence of Ni/SiO_2 microsphere catalysts operated in identical conditions with the present study [30] (See Supplementary file). Results of both catalysts having 4Ni-1Co loading were close to equilibrium, indicating a significant improvement in activity with Co addition which was among the highlights of the study. A comparison to give a perspective on the extent of activity was given following our previous study [30] and studies conducted with varying WHSV values (See Table 2, in "Catalyst stability test" section) [30, 38–41]. A noticeable decrease in CH_4 and CO_2 conversions was observed for both catalysts with an increasing amount of Co in catalyst structure.

Various factors could influence catalytic activity. Strong interaction between the metal and support was previously stated as the reason for the decline in catalytic

Table 2 Literature comparison of synthesized catalyst

Refs.	Catalyst	Reaction conditions	CH_4 conversion	H_2/Co ratio
[30]	5% Ni/SiO_2 microsphere	750 °C, $CH_4/CO_2/N_2$: 1/1/1 WHSV: 36,000 ml (gcat h)$^{-1}$ TOS:18 h	0.73	0.80
[38]	$Ru_{0.1}Ni_{5.0}/MgAlO_x$	800 °C,$CH_4/CO_2/N_2$:25:25:35 WHSV:10,200 ml (gcat h)$^{-1}$ TOS: 50 h	0.94	1
[40]	$Ni_{15}CeMgAl$	750 °C, CO_2/CH_4:1.04/1 WHSV:48,000 ml (gcat h)$^{-1}$TOS:100 h	0.90	0.85
[41]	5% Ni/SiO_2	750 °C, CH_4/CO_2:1 WHSV:18,000 ml (gcat h)$^{-1}$ TOS:200 h	0.66	0.51
[42]	$6Ni_{0.5}Pd$/ mesoporous Al_2O_3	750 °C CH_4/CO_2/Ar:45:45:10 WHSV:22,400 ml (gcat h)$^{-1}$TOS:100 h	0.86	1.08
This study	Ni/SiO_2&Co	750 °C $CH_4/CO_2/N_2$: 1/1/1 WHSV:36,000 ml (gcat h)$^{-1}$TOS:12 h	0.87	0.84

activity [42]. In our case, a possible interaction between Co and the support was unlikely considering the well-known weak interaction between SiO_2 and metal particles [43, 44].

Activity decline in the case of Co addition might depend on the amount of Co added to catalyst structure. Deactivation occurs via coke deposition with high Co loading while metal oxidation was stated to be the main reason in the case of low Co loadings [45]. As previously mentioned, metal loading of the catalysts in the present study varied around 3% with changing amounts of Co and Ni in the structure, and the highest Co amount was determined as 2.57%. This amount was relatively low and the reason of possible decline could be attributed to metal oxidation. Co is active in its metallic state [44, 46], which explains higher activity when Co is impregnated on the surface rather than embedded inside the core of the microsphere. Hence it was logical to assume an increase in metal oxidation for elevated Co amounts on catalyst (Ni/SiO_2&Co) surface during DRM reaction. However, higher conversion values obtained in the case of impregnation (Ni/SiO_2&Co) for all loading amounts implied the negligible effect of metal oxidation on activity decreases.

The decreasing trend of activity, in the presence of $Ni,Co/SiO_2$, was identical to Ni/SiO_2&Co catalysts. Co addition forming NiCo alloy enables tuning of catalyst reactivity and Co simply functioned to decrease the particle size to an extent and increase resistance to metal oxidation [33]. In other words, Co acted as a promoter rather than active metal when placed in the core of the microsphere. Both catalysts exhibited lower activities in the presence of a high Co amount. These lower activities could be explained by the decrease of Ni rather than the increase of Co in catalyst structure. Considering that DRM rate of Ni was higher than Co [45], the increase of Co in catalyst structure probably led to a decrease in the DRM rate and hence a reduction of activity.

H_2/CO ratio for both 4Ni-1Co catalysts were higher compared to 0.8 value determined for Ni containing silica microspheres in our previous study [30]. This was also among the highlights of the study indicating an improvement in syngas composition (Supplementary file).

Characterization of spent Ni–Co bimetallic microsphere catalysts

Characterization analyses were conducted mainly to validate anti coke property of the catalysts except for XRD, the results of which was evaluated to confirm SiC formation during the reaction. DRM reaction initiates with the decomposition of CH_4, leaving carbon species on the surface, and the reaction proceeds with their removal via CO_2 derived species. Ni's activity for CH_4 decomposition is relatively higher which results in coke deposition through time. A second metal with a high affinity to CO_2, such as Co, is often introduced to suppress coke formation [45]. On the other hand, CO_2 contribution to coke formation gains importance as the reaction proceeds, especially at low pressures. Tuning Co with high affinity towards CO_2 is crucial due to possible coke formation in the presence of elevated Co amounts in catalyst structure.[44]. Hence it was logical to assume some coke formation during DRM.

SEM images of catalysts with the highest (4Ni-1Co) and lowest (1Ni-1Co) activity were illustrated for both catalysts (Ni,Co/SiO_2, Ni/SiO_2&Co) (See Supplementary file Fig. 5). Amorphous carbon occurs in the early stages of reaction. Apart from that, both filamentous carbon and graphene-like carbon types could be observed during the DRM reaction. Catalyst deactivation is mainly occurred due to graphene-like carbon [43]. On the other hand, filamentous carbon was reported as the most visible type in SEM images [33, 46]. The formation of filamentous carbon was previously observed for Ni/SiO_2 microspheres [30]. However, no visible sign of coke formation was observed for the catalysts utilized in this study. SEM results indicated an intact, preserved microsphere structure due to Co modification.

Raman spectroscopy was conducted to detect amorphous and/or graphene-like carbon formation. No peaks indicating carbon formation was observed in the wavelength of 1200–1800 cm^{-1}, which was a significant result since both synthesis methods were proven to be effective in terms of stability. Results implied either none or undetectable (below 2%; the threshold of detection for Raman analysis) coke formation during the reaction (See Supplementary file Fig. 6).

TGA analyses of spent catalysts (See Supplementary file Fig. 7) revealed 2 weight loss and 1 weight gain regions, common for all catalysts. Temperature ranges of these regions varied as 25–100, 100–200, and 550–900 °C, respectively. Initial weight loss was due to the removal of adsorbed water from the catalyst. Oxidation of active nickel and cobalt particles during the reaction was the reason of weight gain observed in TGA profiles. The weight loss, which started at 550/600 °C and proceeded up to 900 °C, corresponded to the removal of carbon by burning. Carbon deposition values of the catalysts, determined from weight loss values, were 0.2, 1.5, 0.45 and 0.7%, for 4Ni-1Co, 2Ni-1Co, 1Ni-2Co and 1Ni-1Co, respectively. These values were determined as 0, 0.4, 0.55 and 0.4% for Ni/SiO_2&Co catalysts. Carbon deposition values indicated that the impregnation of Co instead of simultaneous encapsulation had been more effective in preventing coke formation.

Negligible coke formation in the presence of both catalysts (Ni,Co/SiO_2, Ni/SiO_2&Co) was mainly due to crystal sizes. These were determined as 5.2 and 7.9 nm for Ni,Co/SiO_2 and Ni/SiO_2&Co catalysts, respectively. Co addition in the core of microsphere, shattered nickel particles reducing their integrity. As a result, a decrease in particle size with Co addition was observed for Ni,Co/SiO_2 catalysts [33]. Crystalline sizes for both catalysts were below 8 nm, which was previously stated as the threshold of crystal size to achieve coke suppression [47].

Microsphere formation was stated as another critical factor in preventing sintering of the catalysts and enabling coke suppression during DRM reaction [43]. Shell formation around nano alloy particles prevents sintering of active metal in the core and maintains configuration of fine particles with uniform crystal size [48]. That was also the case in our study with close values obtained for crystal sizes in XRD analyses (Fig. 3).

XRD analyses of spent catalysts were conducted to validate SiC formation during DRM reaction. SiC formation was stated as a unique situation with the effect on coke suppression, in our previous studies [30, 31]. Spent catalyst samples were treated with N_2 at 1200 °C for 16 h prior to analyses. Heat treatment converted amorphous silica to crystal β-form enabling detection with XRD.

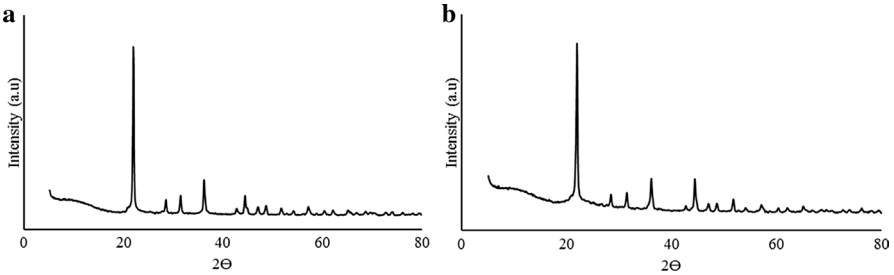

Fig. 3 XRD patterns of the spent catalysts with 4Ni-1Co loading: **a** Ni,Co/SiO_2 synthesized by sol–gel microencapsulation with Ni and Co encapsulated in the core and **b** Ni/SiO_2,Co synthesized by sol–gel microencapsulation-impregnation with Ni encapsulated in the core, Co impregnated on the shell

Cubic SiC structure was validated by XRD peaks obtained at 2θ: 22.4°, 28.9°, 31.8°, 36.8°, 42.8°, 44.6°, 48.8°, 51.9°, 57.2°, 60.3°, 65.4°, 72.7° and 76.4° values (Ref. Code 98–002-4217) (See Supplementary file Fig. 8 for all patterns.).

SiC formation could only be possible as long as a carbon source existed in catalyst structure. Coke formation was not detected with SEM and Raman analyses and TGA results revealed negligible coke formation at the end of the reaction. Based on these results, we could state that carbon species formed during reaction had been utilized to form SiC, giving the self-cleaning property of active sites during the reaction. SiC formation was previously investigated with a reaction between a gas mixture and SiO_2 particles. The reaction temperature was varied between 1000–1500 °C and the gas mixture consisted of CH_4, H_2 and Ar as the carrier [49]. DRM reaction also utilized the same reactants with N_2 as the carrier gas and it was logical to expect SiC formation at 750 °C in these relatively close conditions. SiC formed according to reaction (5) between SiO_2 and C ($SiO_2(s) + 3C(s) \rightarrow SiC\ (s) + 2CO\ (g)$). Although 750 °C was lower than stated onset (1000 °C), CO partial pressures lower than atmospheric pressure could enable SiC formation at lower temperatures as in the case of DRM reaction conducted in this study [50].

Carbon, utilized in SiC formation, was supplied as a result of CH_4 cracking [49], which was also the first step in the DRM reaction. Ni, as a catalyst, was a great candidate for use in SiC production with its high affinity towards CH_4. Co addition, in elevated amounts, considering its high affinity towards CO_2, would increase the rate of Boudard reaction especially at atmospheric pressures. Typically, this should result in coke formation for any catalyst. However, coke amounts obtained in the presence of both (Ni,Co/SiO_2, Ni/SiO_2&Co) catalysts were negligible, and based on these findings, it was logical to assume utilization of multiple carbon sources during SiC formation. This property of the catalyst, to catalyze SiC formation, enabled self-cleaning of the active sites as the reaction proceeded. Self-cleaning would be a useful feature to maintain stable activity, mainly when the reaction was conducted for extended time intervals.

Catalyst stability test

Synthesis procedures were designed to vary the position of Co in catalyst structure, which also affected the role of metal in the DRM reaction. The activity comparison of catalysts revealed higher CH_4 conversions in the case of Co impregnation. Co, on the outer surface of the shell, increased activity during the DRM reaction. Co addition in the core resulted in the decrease of crystal sizes which was previously stated to be crucial in coke suppression. Crystalline sizes for both catalysts were below threshold [47] and coke amounts for Ni/SiO_2&Co catalysts were lower than Ni,Co/SiO_2 catalysts. This result was due to low metal loadings (3%) keeping crystalline sizes in the vicinity of threshold values. Based on the results obtained from reaction experiments and characterization analyses, Ni/SiO_2&Co catalyst with 4Ni-1Co ratio was selected for use in time on stream experiment.

Reaction experiment was conducted in identical conditions ($CH_4/CO_2/N_2$: 1/1/1; 750 °C, 0.1 g catalyst loading.), and results were illustrated in terms of CH_4 and CO_2 conversions in Fig. 4. Conversion values at the end of 12 h were determined as 87 and 93%, respectively. As previously mentioned, activity values for Ni/SiO_2&Co, catalysts were determined as 87 and 94%. Results indicated a constant activity and H_2/CO ratio (0.84) for the investigated time interval. This continuous activity was a substantial improvement considering 5% decrease in the presence of Ni/SiO_2 microspheres, in our previous study [30]. SEM images of spent catalysts taken after 12 h of reaction revealed a stable structure with no visible coke formation (See Supplementary file Fig. 9).

The performance of Ni/SiO_2&Co catalysts with 4Ni-1Co loading was compared with catalysts previously utilized in literature with similar experimental conditions. We intended to give a perspective on the extent of activity and stability of Ni/SiO_2&Co catalyst (Table 2). Although a comparison should be made in identical conditions, it would be logical to state that the CH_4 conversion obtained in the present study was comparable to literature considering lower values obtained in lower WHSV values [30, 41, 42]. The activity of the catalyst could be enhanced by using different types and amounts of metals, as in the case of 31 and 33 which indicated higher values compared to this study. In our opinion, maintaining a stable activity should be the goal in synthesizing catalysts for use in the DRM reaction. A comparison of carbon deposition in these studies revealed variant coke values ranging from 6–49% [38, 40, 41] along with different types of coke formation [42]. Based on this

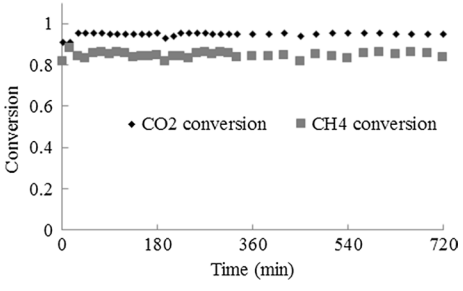

Fig. 4 Stability test at 750 °C, CH_4:CO_2:N_2 = 1:1:1, 0.1 g catalyst loading and WHSV:36,000 ml (gcat h)$^{-1}$ for 12 h, in the presence of Ni/SiO_2&Co catalyst (4Ni-1Co) synthesized by sol–gel microencapsulation-impregnation with Ni encapsulated in the core, Co impregnated on the shell

knowledge, the results of this study could be interpreted as comparable in terms of catalyst activity and stability (2% carbon formation).

Conclusion

DRM reaction was conducted in the presence of Ni,Co/SiO_2 and Ni/SiO_2&Co catalysts with varying Ni and Co loading amounts. Catalysts synthesized with a threshold ratio of 4Ni-1Co was shown to enhance activity compared to Ni containing microsphere catalysts. Conversion values were close to equilibrium, which was among the highlights of the study. Results indicated a decrease of activity with increasing Co loading in catalyst structure. Higher values obtained with Co impregnation (Ni/SiO_2&Co) implied contribution of Co in catalyst activity while Co was useful as a promoter in the presence of Ni,Co/SiO_2 catalysts. Both synthesis procedures were effective in the suppression of coke during DRM. This result was due to the microsphere structure and small crystalline sizes of active materials. Microsphere structure enabled the capture of active material with uniform crystal size and prevented sintering during the DRM reaction. Crystal sizes obtained for both catalysts were lower than the threshold allowing the decrease of carbon nucleation on active sites.

SiC formation was among the highlights of the present study and was introduced as another possible reason for the elimination of coke during DRM reaction. Carbon, generated as a result of methane decomposition, was utilized in SiC formation, which prevented carbon nucleation on active sites and hence suppressed coke formation. Lower coke values were obtained in the presence of Ni/SiO_2&Co catalyst in which Co acted as an activity enhancer. Based on this result, Co was concluded to be a separate carbon source due to its high affinity towards CO_2.

Ni/SiO_2&Co catalyst with the highest activity (4Ni-1Co) was selected for the long-term stability test based on the results of reaction experiments and characterization analyses. Results obtained at the end of 12 h indicated identical activity values compared to 3 h of reaction which was also among the highlights of the study. Synthesis of a catalyst with high activity, outstanding stability and a reasonable chance for industrial application was concluded to be an essential contribution to literature.

Funding This work was supported by Bilecik Seyh Edebali University Research Funds; BAP (2016-02.BŞEÜ.03-07) and BAP (2018-02.BŞEÜ.03-02).

References

1. Zhang J, Wang H, Dalai AK (2007) Development of stable bimetallic catalysts for carbondioxide reforming of methane. J Catal 249:300–310
2. San-Jose-Alonso D, Juan-Juan J, Illan-Gomez M, Roman Martınez M (2009) Ni, Co and bimetallic Ni-Co catalysts for the dry reforming of methane. Appl Catal A 371:54–59

3. Rahemi N, Haghighi M, Babaluo AA, Jafari MF, Estifaee P (2013) Plasma assisted synthesis and physicochemical characterizations of Ni-Co/Al_2O_3 nanocatalyst used in dry reforming of methane. Plasma Chem Plasma Process 33:663–680
4. Xu J, Zhou W, Li Z, Wang J, Ma J (2009) Biogas reforming for hydrogen production overnickel and cobalt bimetallic catalysts. Int J Hydrog Energy 34:6646–6654
5. Aldashukurova G, Mironenko A, Mansurov Z, Shikina N, Yashnik S, Ismagilov Z (2011) Carbon dioxide reforming of methane over Co-Ni catalysts. In: Klemes JJ, Varbanov PS, Lam HL (eds) In: 14th International conference on process integration, modelling and optimisation for energy saving and pollution reduction, pp 63–8
6. Zhu J, Peng X, Yao L, Shen J, Tong D, Hu C (2011) The promoting effect of La, Mg, Co and Zn on the activity and stability of Ni/ SiO_2 catalyst for CO_2 reforming of methane. Int J Hydrog Energy 36:7094–7104
7. Arbag H, Yasyerli S, Yasyerli N, Dogu G (2010) Activity and stability enhancement of Ni-MCM-41 catalysts by Rh incorporation for hydrogen from dry reforming of methane. Int J Hydrog Energy 35:2296–2304
8. Yasyerli S, Filizgok S, Arbag H, Yasyerli N, Dogu G (2011) Ru incorporated Ni-MCM-41 mesoporous catalysts for dry reforming of methane: effects of Mg addition, feed composition and temperature. Int J Hydrog Energy 36:4863–4874
9. Arbag H, Yasyerli S, Yasyerli N, Dogu T, Dogu G (2013) Coke minimization in dry reforming of methane by Ni based mesoporous alumina catalysts synthesized following different routes: effects of W and Mg. Top Catal 56:1695–1707
10. Hou Z, Chen P, Fang H, Zheng X, Yashima T (2006) Production of synthesis gas via methane reforming with CO_2 on noble metals and small amount of noble (Rh-) promoted Ni catalysts. Int J Hydrog Energy 31:555–561
11. Zumreoglu-Karan B, Ay A (2012) Layered double hydroxides multifunctional nanomaterials. Chem Pap 66:1–10
12. He J, Wei M, Li B, Kang Y, Evans DG, Duan X (2006) Preparation of layered double hydroxides. Springer, New York, pp 89–119
13. Nalawade P, Aware B, Kadam V, Hirlekar R (2009) Layered double hydroxides: a review. J Sci Ind Res 68:267–272
14. Tonelli D, Scavetta E, Giorgetti M (2013) Layered-double-hydroxide modified electrodes: electro analytical applications. Anal Bioanal Chem 405:603–614
15. Li F, Duan X (2006) Applications of layered double hydroxides. Springer, New York, pp 193–223
16. Fan G, Li F, Evans DG, Duan X (2014) Catalytic applications of layered double hydroxides: recent advances and perspectives. Chem Soc Rev 43:7040–7066
17. Takehira K, Shishido T, Wang P, Kosaka T, Takaki K (2004) Autothermal reforming of CH_4 over supported Ni catalysts prepared from Mg-Al hydrotalcite-like anionic clay. J Catal 221:43–54
18. Bhattacharyya A, Chang VW, Schumacher DJ (1998) CO_2 reforming of methane to syngas I: evaluation of hydrotalcite clay derived catalysts. Appl Clay Sci 13:317–328
19. Long H, Xu Y, Zhang X, Hu S, Shang S, Yin Y (2013) Ni-Co/ Mg-Al catalyst derived from hydrotalcite-like compound prepared by plasma for dry reforming of methane. J Energy Chem 22:733–739
20. Zamorategui A, Sugita S, Zarraga R, Tanaka S, Uematsu K (2012) Evaluation of dispersibility of gamma alumina prepared by homogeneous precipitation. J Ceram Soc Jpn 120:290–294
21. Feng JT, Lin YJ, Evans DG, Duan X, Li DQ (2009) Enhanced metal dispersion and hydride chlorination properties of a Ni/Al_2O_3 catalyst derived from layered double hydroxides. J Catal 266:351–358
22. Guil-Lopez R, Navarro RM, Pena MA, Fierro JLG (2011) Hydrogen production by oxidative ethanol reforming on Co, Ni and Cu ex-hydrotalcite catalysts. Int J Hydrog Energy 36:1512–1523
23. Bian Z, Kawi S (2017) Highly carbon-resistant Ni-Co/SiO_2 catalysts derived from phyllosilicates for dry reforming of methane. J CO2 Util 18:345–252
24. Silva CKS, Baston EP, Melgar LZ, Bellido JDA (2019) Ni/Al_2O_3-La_2O_3 catalysts synthesized by a one-step polymerization method applied to the dry reforming of methane: effect of precursor structures of nickel, perovskite and spinel. Reac Kinet Mech Cat 128:251–269
25. Bouarab R, Akdim O, Auroux A, Cherifi O, Mirodatos C (2004) Effect of MgO additive on catalytic properties of Co/SiO_2 in the dry reforming of methane. Appl Catal A 264:161–168

26. Swirk K, Galvez ME, Motak M, Grzybek T, Ronning M, Da Costa P (2019) Syngas production from dry methane reforming over yttrium-promoted nickel-KIT-6 catalysts. Int J Hydrog Energy 44:274–286
27. Erdogan B, Arbag H, Yasyerli N (2015) SBA-15 supported mesoporus Ni and Co catalysts with high coke resistance for dry reforming of methane. Int J Hydrog Energy 43:1396–1405
28. Al-Fatesh As, Arafat Y, Atia H, Ibrahim AA, Ha QLM, Schneider M, M-Pohl M, Fakeeha AH (2017) CO_2 reforming of methane to produce syngas over Co-Ni/SBA-15 catalyst: effect of support modifiers (Mg, La and Sc) on catalytic stability. J CO2 Util 21:395–404
29. Wang Y, Fang Q, Shen W, Zhu Z, Fang Y (2018) (Ni/$MgAl_2O_4$)@SiO_2 core-shell catalyst with high resistance for the dry reforming of methane. Reac Kinet Mech Cat. https://doi.org/10.1007/s11144-018-1404-2
30. Gunduz-Meric G, Arbag H, Degirmenci L (2017) Coke minimization via SiC formation in dry reforming of methane conducted in the presence of Ni-based core–shell microsphere catalysts. Int J Hydrog Energy 42:16579–16588
31. Gunduz-Meric G, Degirmenci L (2018) Validation of consecutive coke and SiC formation on Ni core-shell microspheres during methane decomposition. Catal Lett 148:2127–2132
32. Xu L, Wang F, Chen M, Fan X, Yang H, Nie D, Qi L (2017) Alkaline-promoted Co-Ni bimetal ordered mesoporous catalysts with enhanced coke-resistant performance toward CO_2 reforming of CH_4. J CO2 Util 18:1–14
33. Djinovic P, Crnivec I, Erjavec B, Pintar A (2012) Influence of active metal loading and oxygen mobility on coke-free dry reforming of Ni-Co bimetallic catalysts. Appl Catal B 125:259–270
34. Goicoechea S, Kraleva E, Sokolov S, Schneider M, Pohl M, Kockmann N, Ehrich H (2016) Support effect on structure and performance of Co and Ni catalysts for steam reforming of acetic acid. Appl Catal A 514:182–191
35. Degirmenci L, Orbey N (2013) Microencapsulation of silicotungstic acid to retain catalytic activity. Ind Eng Chem Res 52:16714–16718
36. Arbag H, Yasyerli S, Yasyerli N, Dogu G, Dogu T, Crnivec IGO (2015) Coke minimization during conversion of biogas to syngas by bimetallic tungsten-nickel incorporated mesoporous alumina synthesized by the one-pot route. Ind Eng Chem Res 54:2290–2301
37. Sing KSW, Everett DH, Haul RAW, Moscou L, Pieroti RA, Rouquerol J, Siemieniewska T (1985) Reporting physisorption data for gas/solid systems with special reference to the determination of surface area and porosity. Pure Appl Chem 57(4):603–619
38. Tsyganok AI, Inaba M, Tsunoda T, Uchida K, Suzuki K, Takehira K, Hayakawa T (2005) Rational design of Mg-Al mixed oxide-supported bimetallic catalysts for dry reforming of methane. Appl Catal A 292:328–343
39. Bao Z, Lu Y, Han J, Li Y, Yu F (2014) Highly active and stable ni-based bimodal pore catalyst for dry reforming of methane. Appl Catal A. https://doi.org/10.1016/j.apcata.2014.12.005
40. Wang F, Xu L, Shi W (2016) Syngas production from CO_2 reforming with methane over core-shell Ni@SiO_2 catalysts. J CO2 Util 16:318–327
41. Ma Q, Sun J, Gao X, Zhang J, Zhao T, Yoneyama Y, Tsubaki N (2016) Ordered mesoporous alumina supported bimetallic Pd-Ni catalysts for methane dry reforming reaction. Catal Sci Technol. https://doi.org/10.1039/C6CY00841K
42. Ay H, Uner D (2015) Dry reforming of methane over CeO_2 supported Ni, Co and Ni-Co catalysts. Appl Catal B 179:128–138
43. Zhao X, Li H, Zhang J, Shi L, Zhang D (2016) Design and synthesis of NiCe@m-SiO_2 yolk-shell framework catalysts with improved coke-and sintering resistance in dry reforming of methane Int J Hydrog Energy. https://doi.org/10.1016/j.ijhydene.2015.10.111
44. Wu H, Liu J, Liu H, He D (2019) CO_2 reforming of methane to syngas at high pressure over bi-component Ni-Co catalyst: the anti-carbon deposition and stability of catalyst. Fuel 235:868–877
45. AlSabban B, Falivene L, Kozlov SM, Aguilar-Tapia A, Ould-Chikh S, Hazemann JL, Cavallo L, Basset JM, Takanabe K (2017) In-operando eluciation of bimetallic CoNi nanoparticles during high-temperature CH_4/CO_2 reaction. Appl Catal B 213:177–189
46. Arbag H, Yasyerli S, Yasyerli N, Dogu G, Dogu T (2016) Enhancement of catalytic performance of Ni based mesoporous alumina by Co incorporation in conversion of biogas to synthesis gas. Appl Catal B 198:254–265
47. Hin J, Cui H, Cheng Z, Zhou Z (2018) Bimetallic Ni-Co/SBA-15 catalysts prepared by urea co-precipitation for dry reforming of methane. Appl Catal A 554:95–104

48. Wu T, Cai W, Zhang P, Song X, Gao L (2013) Cu-Ni@SiO_2 alloy nanocomposites for methane dry reforming catalysis. RSC Adv 3:23976–23979
49. Ksiazek M, Tangstad M, Dalaker H, Ringdalen E (2014) Reduction of SiO_2 to SiC using natural gas. Metall Mater Trans E 1:272–279
50. Li X, Zhang G, Tang K, Ostrocski O, Tronstad R. Synthesis of Silicon carbide by carbothermal reduction of quartz in H_2-Ar gas mixtures. In: The Fourteenth International Ferroalloys Congress, pp 548–534